

Health Monitoring Using MWM[®]-Array and IDED[®]-Array Sensor Networks

David Grundy, Andrew Washabaugh, Darrell Schlicker, Ian Shay, Neil Goldfine

JENTEK Sensors, Inc., 110-1 Clematis Avenue, Waltham, MA 02453-7013

Ph: 781-642-9666, Fax: 781-642-7525, Email: jentek@shore.net

Abstract

This paper describes the use of MWM eddy current array sensor networks and IDED dielectrometer array sensor networks as well as hybrid MWM-IDEED sensor networks for monitoring of absolute electrical properties for the purposes of detecting and monitoring damage, usage and precursor states within an Adaptive Damage Tolerance (ADT) framework. We present specific results from MWM-Array fatigue monitoring demonstrations, temperature measurement and dynamic stress monitoring, along with IDED methods for age degradation monitoring. We also describe the use of such sensor networks as part of an ADT framework, as well as for generation of real damage standards (e.g., real cracks without starter notches), and for prognostics model validation.

1. INTRODUCTION

On-aircraft damage and usage monitoring is needed for both legacy and new aircraft to achieve cost-effective condition based maintenance. Information obtained from sensors that monitor the material condition enable predictions of damage evolution. Sensors can focus on detection of damage, e.g. cracks, corrosion, and composite delamination, as well as usage monitoring of usage states, such as the stress/loads and temperature/cumulative thermal exposure [1-5]. Measurements of the material conditions and usage states can then be used, to prompt nondestructive testing/inspections, repair/rework/replace actions, and operational decisions for structures [6]. While the sensors may be placed in critical or high stress locations to provide early indications of damage, in other situations there is the potential for general or widespread material property changes and numerous sensors are necessary to provide adequate monitoring of the entire material. To remain cost effective, these sensors should be configured into networks and be low cost and durable. A self-diagnostic capability is also essential to avoid false damage indications.

Electromagnetic sensors are well suited to material condition assessment and health monitoring. Low frequency measurements, in the quasistatic regime, allow the material to be tested preferentially by electric or magnetic fields. Electric field based (i.e., capacitive, or dielectrometry) sensors permit measurements of insulating and weakly conducting materials [5]. Magnetic field, (i.e. inductive, or eddy current sensors) are suitable for conducting and/or magnetic materials [1]. Low frequency operation along with attention to the electrode or winding design provides sensors whose response can be modeled accurately. This can relax calibration requirements and permits calibration information to be recalled when plugging into the sensor prior to performing a measurement. This is also useful for leave-in-place sensors where it is important to be able to perform self-diagnostics on the sensor to determine if it is still operating correctly. For example, the lift-off (proximity) of the sensor to the surface might be monitored at each successive measurement to verify that the sensor is functioning and has not moved since the last measurement. Also, applied or ambient variations, such as temperature changes, produce predictable changes in the absolute material properties, e.g. conductivity, such that variations in such absolute properties can be monitored to verify performance of absolute sensors in place [patents issued and pending].

Typically, the condition monitoring needs to be performed at multiple locations on a structure. In some cases, this can be accomplished using a sensor array with multiple sensing elements. For example, crack propagation can be monitored as the crack passes underneath individual sense elements [7]. In other cases, the monitored locations may be relatively far apart and numerous sensors or sensor arrays are required. This paper describes some quasistatic electric and magnetic field sensor arrays, along with some examples, for material condition monitoring.

2. IDED AND MWM SENSORS

The sensing mode selection depends upon the properties of the material to be inspected. For insulating or dielectric materials, electric field based sensors such as the Interdigitated Electrode Dielectrometer (IDED) can be used. In contrast, for conducting or magnetic materials, magnetic field based sensors such as the Meandering Winding Magnetometer (MWM) can be used. For both the IDED and MWM, the sensor response to layered media can be accurately modeled and used to provide absolute property measurements. These sensors, along with the inversion of the sensor response into material properties, are reviewed in this section.

The basic structure for the capacitive IDED sensor is shown in Figure 1(a). One set of electrode fingers are driven by a sinusoidally time varying signal with known amplitude and the second set of interdigitated fingers are virtually grounded, with the terminal current constituting the sensed signal. For layered media or materials having dielectric properties that vary with depth, the measured transadmittance between the drive and sense electrode, or the effective complex permittivity of the material, is a thickness and depth-weighted response of the dielectric properties of the various regions. Typical excitation frequencies range from 0.005 Hz for highly insulating materials to 10 MHz for semiconducting materials. An example IDED sensor and enclosure are shown in Figure 1(b).

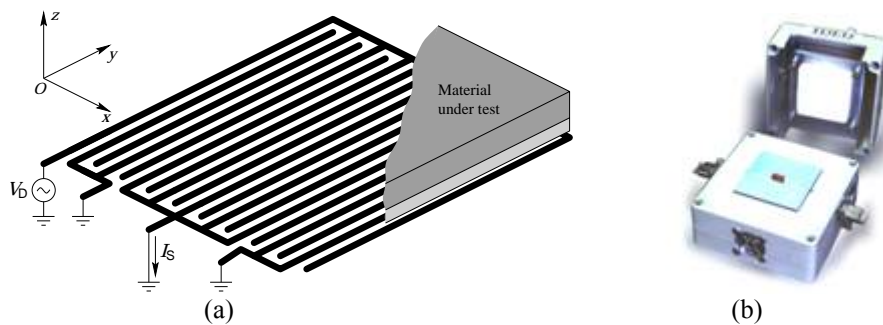


Figure 1: (a) IDED sensor in contact with a test material; and (b) commercially available sensor and enclosure for capacitive sensing of dielectric samples.

For the IDED, the depth of penetration of the electric field into the material is proportional to the spatial wavelength of the periodic electrodes. The periodic variation of electric potential along the surface in the x direction (of Figure 1(a)) produces an exponentially decaying electric field that penetrates into the medium in the z direction. The depth of sensitivity is considered to be approximately $\frac{1}{3}$ of the fundamental spatial wavelength. This implies that small wavelength sensors will primarily respond to changes of material properties near the sensor-material interface, while larger wavelength sensors respond to changes farther from the sensor interface. Thus multiple wavelength sensors can be used to measure spatial profiles of dielectric properties [8]. Unlike the magnetic sensors, where the depth of sensitivity can be controlled by changing the drive frequency, acquiring the necessary information to estimate multiple unknowns with the IDED can be accomplished via different spatial wavelengths or segmented fields [patents issued and pending].

Several types of multiple wavelength sensors have been developed. In one approach, multiple sets of interdigitated spatially periodic electrodes are laid out on a common substrate, as shown in Figure 2(a), and placed in proximity to the test specimen. While this provides distinct wavelength IDEDs, each IDED is sensitive to different regions of the test material. As a result, if there is a spatial variation in the thickness or dielectric properties of the test material, or if there is an air gap variation, for example, due to uneven pressure against the material or dust particles, it can be difficult to combine the measurements for meaningful property estimates. A solution is to integrate multiple sensing elements into a single sensing structure so that all of the sensing elements interrogate the same region of the material under test, as

illustrated in Figure 2(b) [9]. A schematic for the electric field distribution is shown in Figure 3, where multiple sensing electrodes are placed within each interdigitated electrode period and respond to different effective wavelength (short or long) modes of the electric field. Thus, for this sensor, the lift-off and dielectric constant can be measured independently. For layered materials, including the air gap, more sense elements can be incorporated into the IDED to sense other segments of the field distribution. Figure 2(c) shows an example segmented-field IDED with three effective wavelengths. Circular versions of this approach have also been demonstrated [5]. This multiple wavelength sensing approach can also be extended to include multiple distinct elements. An example is shown in Figure 4. Each element spans three spatial periods of the periodic electric field. At each channel location, the material is probed at three depths using the segmented-field approach.

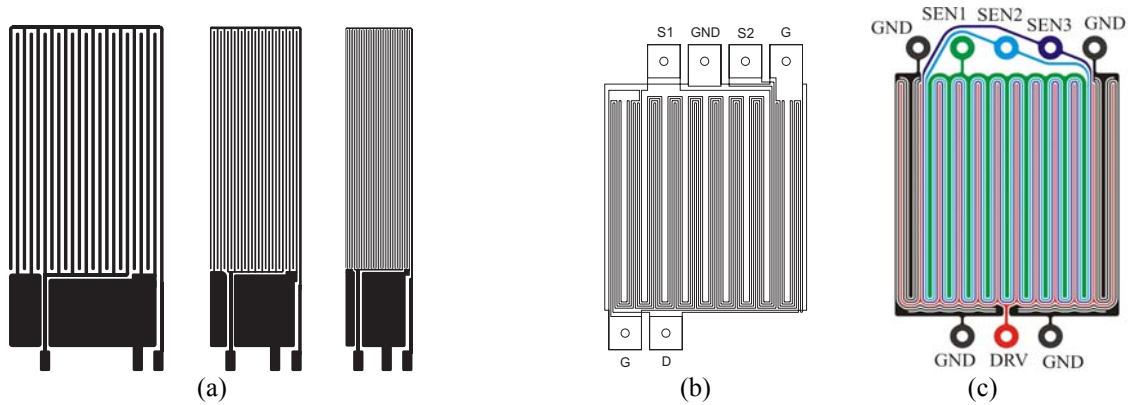


Figure 2: (a) A three-wavelength sensor with three separate sensing regions of different wavelength formed on a Teflon substrate with wavelengths of 5 mm, 2.5 mm, and 1 mm. Schematics for co-located IDED's having (b) two and (c) three wavelengths.

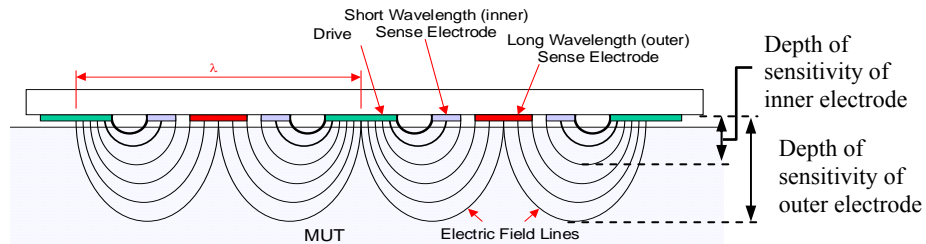


Figure 3: Multiple co-located dielectric sensors sense the same region of the test material, ensuring that the longer and shorter wavelengths have the same average lift-off or air gap thickness.

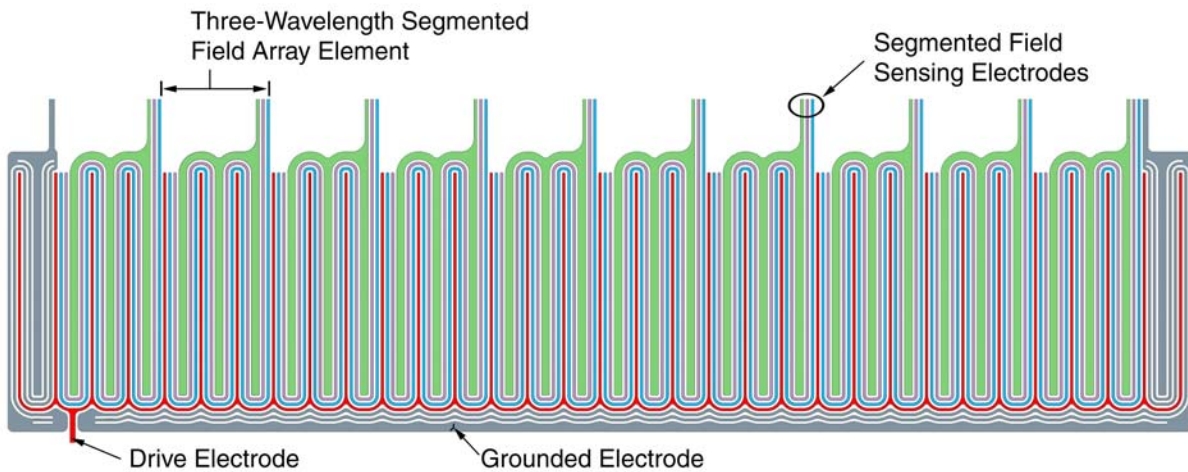


Figure 4: Schematic diagram of a three-wavelength, ten element, IDED-Array.

The MWM is an inductive, eddy-current-based sensor that is designed specifically for the nondestructive characterization of material properties in the near-surface region (within 0.35 in.) [1,10,11]. As shown in Figure 5 (a), the sensor has a meandering primary winding for creating the magnetic field and secondary windings located on opposite

sides of the primary for sensing the response. The windings are typically mounted on a thin and flexible substrate, producing a conformable sensor. Micro-fabrication techniques are employed to produce the sensors, resulting in highly reliable and highly repeatable (i.e., essentially identical) sensors. Connections can be made to individual sense elements, as shown in Figure 5(b) typically for surface mounted applications, or the sense elements can be subdivided into smaller elements in the y -direction for creating property images when scanned in the x -direction. The MWM sensor was designed to produce a spatially periodic magnetic field. The winding pattern permits the sensor response to be accurately modeled with rapid computational methods and to provide dramatically reduced calibration requirements. For example, in some situations an "air calibration" can be used to measure a component's absolute electrical conductivity without calibration standards [12]. For coating applications, calibration is only required on a reference part having the approximate properties of the substrate. Coated standards are not required.

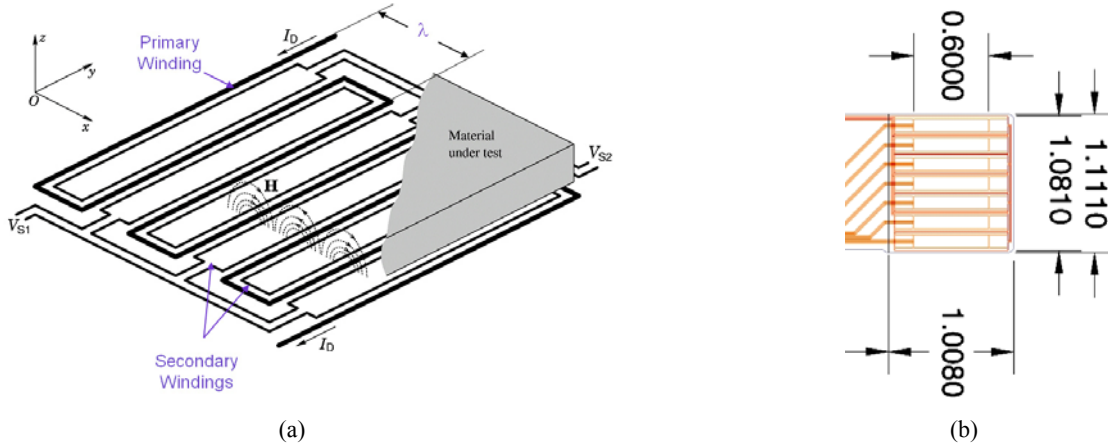


Figure 5: (a) Single sensing element MWM-sensor design. (b) A linear MWM-Array design.

The IDED (or MWM) response is converted into material or geometric properties using databases of precomputed sensor responses. In two dimensions, this can be visualized as a measurement grid. Measurement grids map the magnitude and phase of the transmittance (or transimpedance, for the MWM) into unknown properties of interest [1]. The grids are used to calibrate the sensors and perform measurements of absolute materials properties. Typically, grids relate two measured parameters to two unknowns, such as the dielectric constant and lift-off, electrical conductivity and lift-off, or metallic coating thickness and lift-off. For more than three unknowns, higher-dimensional versions of these databases are used. For three unknowns, such precomputed databases are called lattices, while for four or more unknowns they are called hypercubes. The use of such precomputed databases and model based calibration methods enables rapid data processing, robustness, and self-diagnostics [patents issued and pending].

As an example, Figure 6 shows the noncontact measurement of the permittivity of an insulating dielectric material of known thickness. The material is insulating so there is no phase information in the measurement and the magnitudes from two different wavelength-sensing elements are used to create the measurement grid. The grid illustrates the dependence of the sensed magnitudes on the dielectric constant of a material with a known thickness and the air gap between the material under test and the sensor. Sets of data points for two different materials, each 1.58-mm thick, are plotted. The flat and rigid sample materials, Lexan™ and a printed circuit board (PCB) substrate, were suspended above the face of the sensor to simulate noncontact measurements of the materials with various liftoffs or air gaps. For each material, the sample points approximately follow lines of constant dielectric constant.

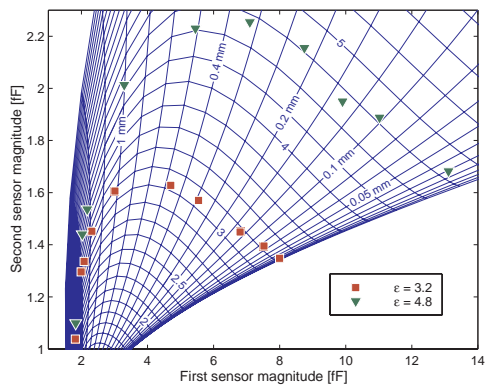


Figure 6: Measurement grid and results of two-unknown measurements carried out with a cylindrical IDED.

Data set	Lexan □		PCB ▽	
	ϵ	h [mm]	ϵ	h [mm]
1	3.20	0.019	4.76	0.029
2	3.22	0.070	4.83	0.100
3	3.18	0.135	4.73	0.139
4	3.15	0.299	4.90	0.213
5	3.14	0.458	4.84	0.325
6	3.30	1.028	4.68	0.497
7	3.46	1.528	4.82	0.984
8	3.49	1.845	4.48	1.662
9	3.57	1.979	4.53	1.865
10	3.60	2.877	3.68	2.641

While conventional nondestructive testing equipment can cope with no more than two variables, such as coating thickness and lift-off, sensor designs whose response can be accurately modeled permit estimation of more than two properties. These estimated properties are determined from measurement values obtained at multiple wavelengths and/or multiple frequencies. As an example, Figure 7 shows a pair of three-dimensional grid lattices, where each grid describes the MWM sensor response to changes in coating thickness and lift-off at a given coating conductivity. The lattices shown in Figure 7 contain coating thickness / lift-off grids for numerous values of the coating conductivity (only four grids are shown here for illustration purposes at 1 MHz and 6.31 MHz). Within each grid, the spacing between the grid points indicates the sensitivity for independently estimating the coating thickness or lift-off. The grid spacing depends on the difference between the coating and substrate conductivities. The lattices of Figure 7, are relatively coarse for visualization purposes, with only 140 lattice points (7 coating thicknesses, 5 lift-offs, and 4 coating conductivities), whereas a typical lattice has on the order of 20,000 points.

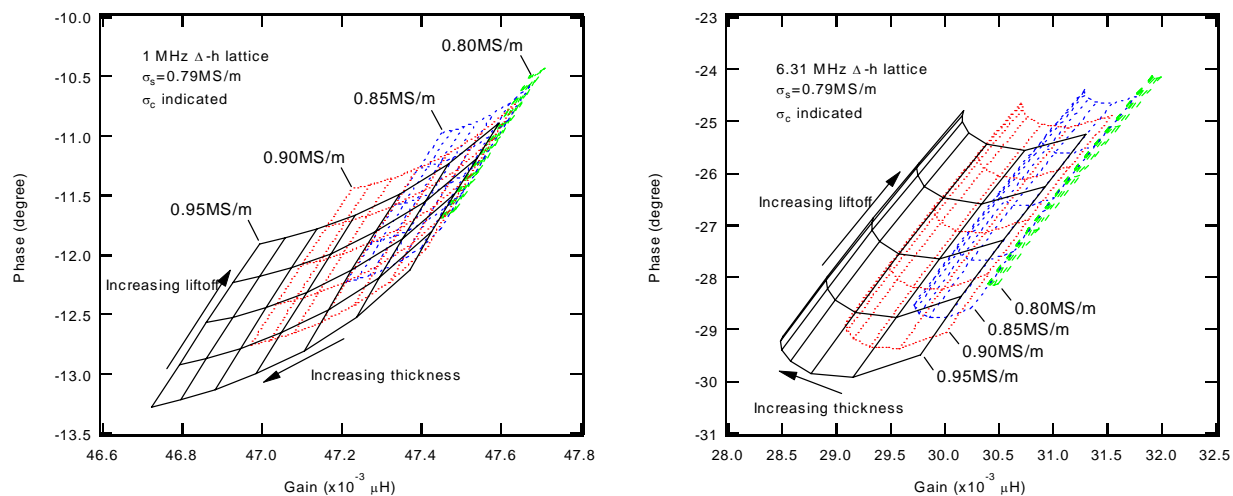


Figure 7: Example MWM coating thickness - lift-off grid lattices for a coating family.

3. REPRESENTATIVE MEASUREMENT APPLICATIONS

Measurements have been performed for numerous applications to demonstrate this sensing method and inversion approach. The following provides some example measurement applications.

Figure 8 shows a representative experiment configuration for demonstrating three-unknown property estimates using a segmented field IDED. In this example, the unknown properties are the lift-off gap thickness and the thickness and permittivity of a coating layer on a dielectric substrate. In this case, it is assumed that all of the materials are insulated so that only the magnitudes from three IDED wavelengths can be used. At a single excitation frequency, this provides three

measurement values from which the unknown properties can be estimated. The inversion results listed in Table 1 show the capability of the approach in determining the properties. The permittivity measurements do not vary with layer thickness, and the thicknesses are within 0.4 mils of the micrometer readings.



Figure 8: Three-unknown measurement setup using a segmented field IDED.

Table 1: Three-unknown measurement results.

Dielectric Material	Reference Relative Permittivity	Thickness* (mils)	Measured Thickness (mils)	Measured Relative Permittivity	Measured Lift-Off (mils)
Teflon	2.0-2.1	6 x 2.9 mils = 17.4 mils	17.71	1.93	0.26
			17.78	1.93	0.26
		7 x 2.9 mils = 20.3 mils	20.61	1.94	0.26
			20.60	1.94	0.27
		8 x 2.9 mils = 23.2 mils	23.24	1.95	0.25
			23.40	1.95	0.26

* Determined by micrometer measurement

An example IDED measurement illustrating structural dielectric property changes is shown in Figure 9. This shows the effect of tensile loading of a glass fiber composite on the relative permittivity. These measurements were made at a single frequency and the decrease in permittivity is consistent with a reduction in the local density of the material, expansion of voids, or degradation (microcracking) of the fiber or matrix. Using the segmented field approach, noncontact measurements can also be performed. Similar measurements have also been used to assess the porosity in ceramics, to detect disbonds or cracks in composite materials, and to monitor moisture ingress [patents issued and pending].

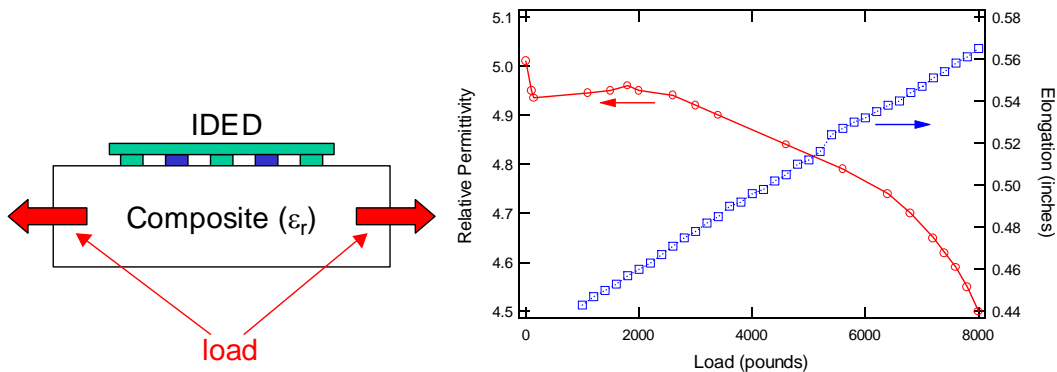


Figure 9: Test geometry and permittivity measurements for a glass fiber composite tensile loading test.

Networks of sensor arrays have also been used to monitor damage initiation and propagation in metallic structures using MWM-Arrays. Figure 10 illustrates a four-hole joint specimen representative of an aircraft structural joint, with embedded MWM-Arrays. Following installation of the MWM-Arrays and bolting the specimen, it was cycled in a load frame to induce fatigue cracking at the fastener holes. The MWM-Arrays successfully detected and monitored crack progression throughout the test and remained functional even after the specimen had failed. **The sensors outlasted the metal.**

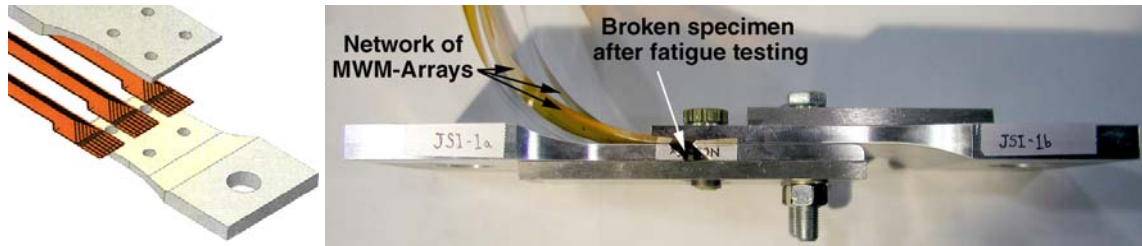


Figure 10: MWM-Arrays were embedded into this 4-hole specimen and successfully monitored crack growth up to specimen failure.

Figure 11 illustrates a ten-hole specimen that was similarly constructed with embedded MWM-Arrays. The MWM-Arrays were mounted between the holes in the lower and upper rows. The equipment set-up with the specimen in the load frame and the JENTEK 37 channel probes are shown in Figure 11(c). The crack tip progression data are shown in Figure 12. The colored lines indicate progression of crack tips from one hole towards another as a function of number of cycles. As in the four hole tests, the MWM-Arrays successfully monitored crack growth throughout the test with the sensors embedded at the buried interface between the metal plates. Again, the sensor outlasted the metal in numerous tests. In fact, once procedures were finalized, no sensors failed in subsequent tests.

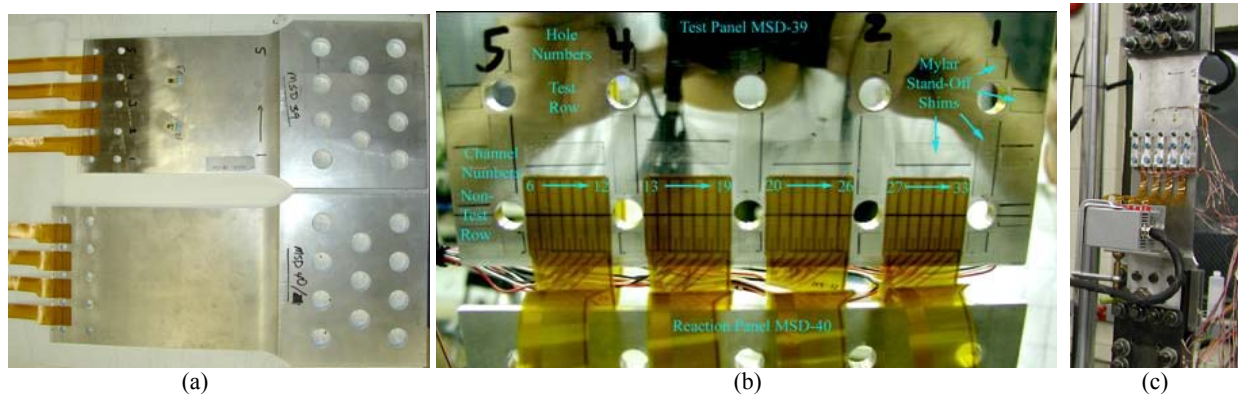


Figure 11: (a) MWM-Arrays mounted along both rows of fastener holes. (b) The ten-hole specimen with embedded MWM-Arrays shown prior to bolting up. (c) The ten-hole specimen is mounted in the load frame in the photo on the right.

Figure 13 shows the use of MWM sensors to monitor the magnetic permeability as a means of dynamically monitoring stress. For these sensors, no mechanical load transfer is required between the material under test and the sensor (as in a strain gauge). For nonferrous metals, a coating with a stress sensitive magnetic permeability is applied. Furthermore, low frequencies can be used to monitor stress variations at buried interfaces, e.g. faying surfaces or at the interface between a roller bearing and the race (i.e., contact stress).

Similarly, temperature can be monitored at buried interfaces, on the surface or on the inside of a component from the outside (i.e., through wall) using multiple frequency methods. For example, the temperature inside an engine might be monitored from the outside by abstractly dividing the case thickness into three layers and estimating the electrical conductivity of each layer. The variation in the electrical conductivity with temperature is then correlated with temperature for each layer. Sensitivity can be enhanced by introducing coatings with enhanced sensitivity to temperature or other properties of interest [patents issued and pending].

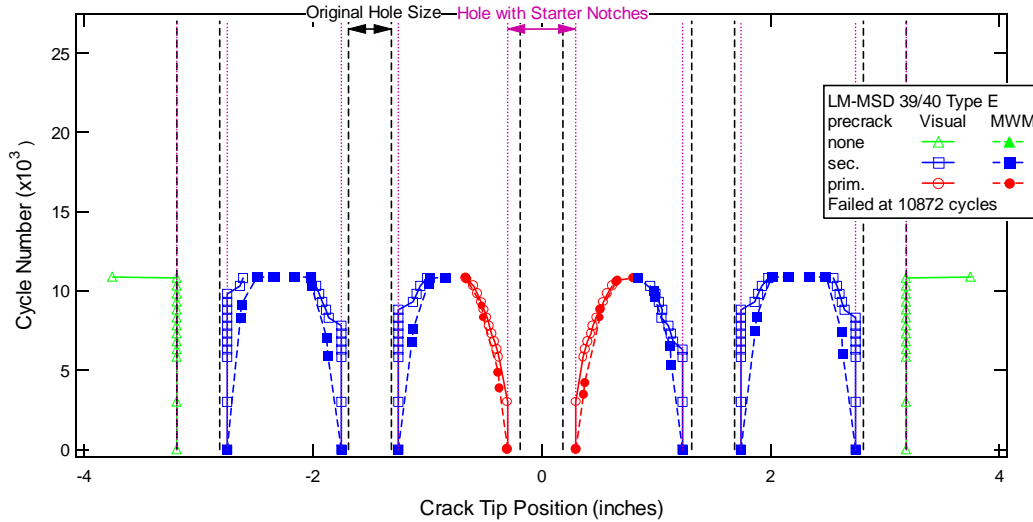


Figure 12: Representative multiple crack growth monitoring data.

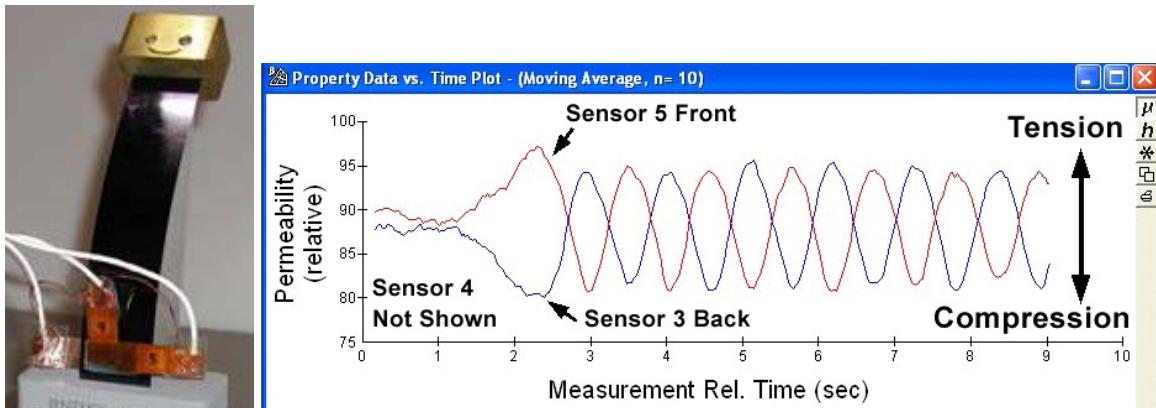


Figure 13. Dynamic stress monitoring for ferrous and nonferrous alloys.

4. SENSOR NETWORKS AND ADT FRAMEWORK

Information about a structure's material condition obtained from networks of sensors or sensor arrays can also be used in a damage tolerance approach. This is best illustrated by an example. Damage tolerance methodologies assume an initial crack size, just below the detection threshold of available nondestructive evaluation (NDE) methods. For example, in a military aircraft structure (e.g., lap joint) a crack growth model is used to predict the progression of the assumed initial crack. The critical crack size is that size at which the component's residual strength reaches the level at which the component is no longer damage tolerant. Inspection intervals are set at a fraction of the time it takes for the assumed initial crack to reach this critical crack size.

In contrast, the Adaptive Damage Tolerance (ADT) approach extends the damage tolerance methodology by adding a model-based adaptation of inspection intervals based on observable precursor, usage and damage states. Figure 14 provides a flow diagram of a possible ADT methodology and means for combining QA, NDE, CBM and PHM for life-cycle management. This framework introduces several new concepts, including: (1) a requirement to provide observability¹ of relevant precursor states², (2) adjustment of unobservable damage state³ assumptions (in the current

¹ **Observability** – is a control theory term, represented for linear multivariate systems by the observability matrix. In this context, observability implies not only the capability to measure specific damage states and their rates of change, but also to measure them independently and reliably.

² **Precursor States** – are defined here as states that affect the early behavior of a specific damage mode. Examples of precursor states are inadequate residual stresses, either as manufactured or as modified in service, undesirable surface conditions (e.g., from

damage tolerance approach the assumption about the initial unobserved crack size is not adjusted) to produce model derived failure statistics representative of observed failures in the fleet or component tests, (3) a framework for combining data from field and depot NDE inspections with data from onboard sensors for monitoring of both usage and damage state progression, (4) adjustment of traditional inspection intervals and onboard sensor data analysis intervals based on progression of damage states and usage i.e., data from on-board sensors might only be downloaded and analyzed at specified, adjustable intervals by selected authorities, as opposed to on-site – to limit the effects of false positive indications on readiness, (5) detecting and accounting for possible upset events⁴, and (6) adaptive recapitalization⁵ through maintenance/rework/repair and replacement actions as a method of introducing health control⁶, i.e., going a step beyond health management, and (7) formulation of a quantitative performance goal incorporating total ownership cost and performance, with feedback from individual component and fleet-wide tracking that might provide the asset health control objective [6].

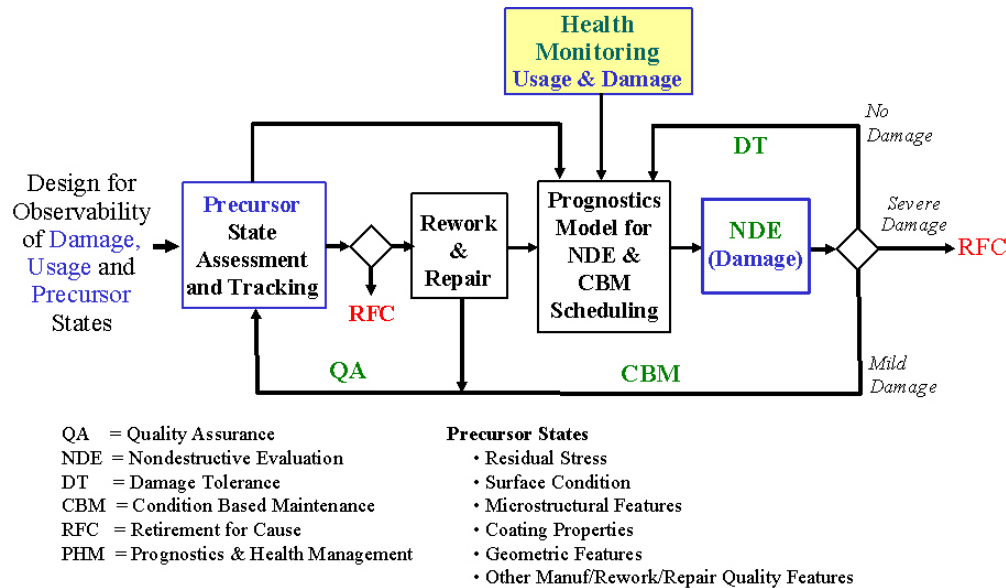


Figure 14: Adaptive damage tolerance flow chart.

The principal distinction between precursor states and damage states is that precursor states result from manufacturing processes and rework/repair events. Characterization of these states may introduce requirements for quality assessment beyond typical practices. Some precursor states, e.g. inadequate residual stress, may be further modified by subsequent in-service damage. For example, a shot peened or otherwise cold worked structural component might have been cold worked to extend high cycle fatigue life, but in practice substantial low cycle fatigue contribution may result in stress relaxation, making the component more susceptible to fatigue crack initiation and propagation.

In some applications, gradual or sudden changes of such precursor states may provide the only sufficiently early warning of subsequent failure, when for example, time between crack initiation and failure is too short. This might be the case in

manufacturing or fretting), geometric features, microstructure variations (e.g., from aggressive machining in titanium engine disks, or from grind burns in low alloy steel components).

³ Unobservable Damage States – are states that cannot yet be monitored nondestructively, but can be included in prognostics models of failure mode progression. Note, however, that the sequential nature of damage behavior may permit the bounding of unobservable conditions through observations that the next stage of behavior has not yet started, e.g., no failures in the fleet might imply that cold working was accomplished correctly for a component population or population subset and that the unobservable damage states are still benign.

⁴ Upset Event – a discrete event that shifts relevant damage states either in a positive or negative direction.

⁵ Adaptive Recapitalization – recapitalization is defined as a means of resetting or at least recovering a substantial portion of the component life through health control actions, such as grinding/blending areas affected by cracks or pits and reshotpeening, or stripping and recoating, expanding a fastener hole, or adding a doubler. Adaptive recapitalization includes adaptation of recapitalization methods based on models of damage progression for specific failure modes of concern, and within mission constraints.

⁶ Health Control- beyond health management, control implies the capability to alter the precursor and damage states using a measured action with a predictable response.

a landing gear where a previous overload event, e.g., hard landing, changed the precursor states, e.g., residual stresses, without producing a detectable crack. For this example, the next overload event may result in a failure of the component. In this case, the focus should be on materials characterization to observe changes in the precursor states, and, when possible, on in-situ monitoring of critical locations using permanently mounted sensors.

One example of a currently used method for monitoring precursor states is the use of the Barkhausen noise method on landing gear. This method is used to remove landing gear components from service if they exhibit unacceptable residual stress conditions. Unfortunately, this method requires costly stripping of paint and produces a substantial number of false positive indications. MWM-Arrays are an alternative method that does not require paint removal and should provide substantial improvements in reliability with reduced false indications. For example, the high-resolution imaging capability of the MWM-Array combined with the capability to perform bidirectional measurements provides the new potential to differentiate between residual stress patterns and microstructural conditions, for example, grinding burns. Despite current limitations, such techniques are becoming more and more prevalent, not only for manufacturing quality control, but also as a means for detecting changes in precursor states to assess fitness for service.

5. SUMMARY

Networks of electroquasistatic or magnetoquasistatic sensors and sensor arrays can provide information about structural material conditions and fitness for service. This information can be used to assess damage, usage and precursor states for the structure and can be incorporated into an adaptive framework for damage tolerance that influences repair and maintenance decisions and permits efficient operation and management of the structure.

REFERENCES

1. Goldfine, N.G., "Magnetometers for Improved Characterization in Aerospace Applications," *Materials Evaluation*, Volume 51, No. 3, pp. 396-405, March 1993.
2. Goldfine, N., Sheiretov, Y., Washabaugh A., and Zilberstein V. (2000), "Materials Characterization and Flaw Detection for Metallic Coating Repairs," *BiNDT Journal Insight*, Vol.42, No.12, pp.809-814.
3. Zilberstein, V., Fisher, M., Grundy, D., Schlicker, D., Tsukernik, V., Vengrinovich, V., Goldfine, N., and Yentzer, T., "Residual and Applied Stress Estimation from Directional Magnetic Permeability Measurements with MWM Sensors," *ASME Journal of Pressure Vessel Technology*, Volume 124, pp. 375-381, August 2002.
4. Shay, I., V. Zilberstein, A. Washabaugh, N. Goldfine, "Remote Temperature and Stress Monitoring Using Low Frequency Inductive Sensing," *SPIE NDE/Health Monitoring of Aerospace Materials and Composites*, San Diego, CA, 2003.
5. Schlicker, D., Shay, I., Washabaugh, A., Goldfine, N., Givot, B., "Capacitive Sensing Dielectrometers for Noncontact Characterization of Adhesives and Epoxies," *Society Plastics Engineer, (SPE) ANTEC Conf.*, 2002.
6. Goldfine, N. and V. Zilberstein, "Nondestructive Evaluation for Condition Based Maintenance and Prognostics & Health monitoring of Legacy and New Platforms," published in the proceedings of the 57th Meeting of the Society for Machinery Failure Prevention Technology, April 2003, pp. 17-30.
7. Washabaugh, A. Zilberstein, V., Schlicker, D., Shay, I., Grundy, D., and Goldfine, N., "Shaped-Field Eddy-Current Sensors and Arrays," *SPIE Structural Health Monitoring Conference*, San Diego, CA, 2002.
8. Melcher, J.R. and Zaretsky, M.C., "Apparatus and Methods for Measuring Permittivity in Materials," *US Patent Number 4,814,690*, March 21, 1989.
9. Goldfine, N.J, Zahn, M., Mamishev, A.V., Schlicker, D.E., and Washabaugh, A.P., "Methods for Processing, Optimization, Calibration, and Display of Measured Dielectrometry Signals using Property Estimation Grids," *U.S. Patent Number 6,380,747*, Apr. 30, 2002.
10. Melcher, J.R., "Apparatus and Methods for Measuring Permeability and Conductivity in Materials Using Multiple Wavenumber Magnetic Interrogations," *US Patent Number 5,015,951*, May 14, 1991.
11. Goldfine, N.J, and Melcher, J.R., "Magnetometer Having Periodic Winding Structure and Material Property Estimator," *U.S. Patent Number 5,453,689*, Sep. 26, 1995.
12. ASTM Standard Practice E2338-04, *Characterization of Coatings Using Conformable Eddy-Current Sensors without Coating Reference Standards*, ASTM International, Book of Standards, Vol. 03, 2004.